LBL-21421
OM-220

Presented at the SPIE's 3rd International Conference on Optics and Electrooptics, Innsbruck, Austria, April 14-18, 1986. To be published in Solar Energy Materials.

Spectroscopic and Electrochemical Studies of Electrochromic Hydrated Nickel Oxide Films

P.C. Yu, G. Nazri,* C.M. Lampert
Applied Science Division
and
Materials and Molecular Research Division
Lawrence Berkeley Laboratory
University of California
Berkeley, CA 94720

*General Motors Research Laboratories
Electrochemistry Department
Warren, MI 48090-9055

July 1986

This work was supported in part by the Assistant Secretary for Conservation and Renewable Energy, Office of Solar Heat Technologies, Solar Buildings Division of the U.S. Department of Energy under Contract No. DE-AC03-76SF00098.

Spectroscopic and Electrochemical Studies of Electrochromic Hydrated Nickel Oxide Films

P.C. Yu, G. Nazri,* C.M. Lampert
Lawrence Berkeley Laboratory
University of California
Berkeley, CA 94720

*General Motors Research Labs
Electrochemistry Department
Warren, MI 48090-9055

ABSTRACT

The electrochromic properties of hydrated nickel oxide thin films electrochemically deposited by anodization onto doped tin oxide-coated glass have been studied by transmittance measurements, cyclic voltammetry, Fourier-transform infrared spectroscopy, and ion-backscattering spectrometry. The spectral transmittance is reported for films switched in both the bleached and colored states. The photopic transmittance (T_p) can be switched from T_p(bleached) = 0.77 to T_p(colored) = 0.21, and the solar transmittance (T_S) can be switched from T_S(bleached) = 0.73 to T_S(colored) = 0.35 Also reported is the near-infrared transmittance (T_{NIR}), which was found to switch from T_{NIR} (bleached) = 0.72 to T_{NIR}(colored) = 0.55 for a film thickness of 500 Å. The bleached condition is noted to have very low solar absorption in both the visible and solar regions. Ion-backscattering spectrometry was performed on the hydrated nickel oxide film, yielding a composition of $NiO_{1.0}$ (dehydrated). Cyclic voltammetry showed that, for films in the bleached or colored state, the reversible reaction is $Ni(OH)_2 \longleftrightarrow NiOOH + H^+ + e^-$. Voltammetry also showed that the switching of the film is controlled by the diffusion of protons, where OH^- plays a role in the reaction mechanism. Analysis of the hydrated nickel-oxide thin films by Fourier-transform infrared spectroscopy revealed that both the bleached and colored states contain lattice water and hydroxyl groups. The surface hydroxyl groups play an important role in the coloration and bleaching of the anodically deposited nickel oxide thin films.

INTRODUCTION

Electrochromic hydrated nickel oxide is important for the development of large-scale optical-switching glazings and electronic information displays, particularly when long memory times and low switching rates are desired. The energy-saving value of an electrochromic optical-switching glazing for architectural applications has been determined to be quite high in some situations[1]. By dynamic control of solar radiation entering a glazing, one can modify natural illumination levels, glare, and heat gain to improve comfort, productivity, and energy conservation. Other uses for electrochromic glazings include automotive and aerospace applications.

Hydrated nickel oxide[2] along with certain other transition metal oxides, such as tungsten oxide (WO_3) and hydrated iridium oxide ($IrO_2 \cdot nH_2O$), exhibit the phenomenon known as electrochromism[3-4]. Electrochromism is the process by which a material can exhibit a reversible color change with applied electric current. Electrochromic materials switch from the uncolored to the colored state by simultaneous ion (usually H^+ or Li^+) and electron injection or ejection. As a result of this injection or ejection, color centers are formed in the material. Color centers produce optical absorption in the visible wavelength region[5]. Both chemical and electronic changes coincide with the optical changes in the material. In some cases, the electronic carrier concentration can be modified considerably, giving rise to infrared modulation[6]. There have been a number of studies on nickel oxide electrodes for battery and fuel cell applications[7]. Except for a few investigations on anodically prepared films[8,9], most films were produced by cathodic or chemical precipitation methods. In this study anodic deposition is used to deposit the electrochromic hydrated nickel oxide. It has been noted that both composition and structure of nickel oxide electrodes depend upon the deposition conditions[10, 11].

In order to classify the operation of the device made from nickel oxide, it is important to discuss its construction. Figure 1 is a schematic cross section of a typical solid-state device. As noted in the insert, three major device configurations exist. The five-layer model is used to demonstrate the device complexity. In this model there is symmetry about the ion conductor (layer 3). Both the electrochromic layer (layer 2) and counter-electrode layer (layer 4, or ion-storage media) exhibit mixed ionic and electronic conduction. These layers are flanked by transparent electronic conductors (layers 1 and 5), such as the doped tin oxide (SnO_2:F,Cl) used in this study. The ionic conductor provides a medium by which ions can be transported between the electrochromic and counter-electrode layers when an external potential is applied. When a potential is applied, coloration or bleaching can occur due to the movement of ions and electrons into or out of the electrochromic layer. For experimental convenience our device utilized a liquid KOH electrolyte, which took the place of both layers 3 and 4. Prior to the development of such a device, it is important to better understand the electrochemical and molecular structure of the electrochromic layer.

In a prior study, we reported chemical results using a sputter Auger microprobe and x-ray photoelectron spectroscopy[12]. In the following experiments further properties are determined by optical spectroscopy, backscattering spectrometry, cyclic voltammetry, and Fourier-transform infrared spectroscopy. The understanding of the reaction mechanism and kinetics gained by integrating the results obtained by several characterization techniques will ultimately aid in device design.

EXPERIMENTAL PROCEDURES

The nickel oxide thin-film samples were electrochemically deposited onto fluorine-doped tin oxide-coated glass. By using a Princeton Applied Research (model 273) scanning potentiostat, a controlled wavefunction was applied to the conductive electrode, where a two-step process was used to prepare the nickel oxide films. The first step was the anodic deposition of the film in a nickel buffer solution, followed by cycling the film in an alkaline solution to study the switching characteristics, all of which were monitored by a X-Y-T recorder, Esterline Angus (model 1117).

The conductive substrate, supplied by Watkins-Johnson Company (Scotts Valley, CA), was based on a tin oxide (SnO_2:F,Cl) coating on glass, produced by atmospheric chemical-vapor deposition involving hydrolysis of $SnCl_4$ and NH_4F[13]. The coating had a sheet resistance of 5 ohms/cm^2. To make electrical contact, a copper wire was attached to this surface with silver epoxy.

The electrolyte used to anodically deposit the nickel oxide films on the conductive glass was a solution of 0.1M $NiSO_4 \cdot 6H_2O$ and 0.1M NH_4OH (analytical grade, Fisher Scientific Co.) at 23 °C. The solution was magnetically stirred for 5-10 minutes. The glass electrode was then cycled from -500 to +1500 mV vs. SCE (standard calomel electrode) at a potential sweep rate of 20 mV/ sec. The nickel oxide was deposited on the glass with each anodic cycle, and after five cycles, the deposition rate decreased due to an increase in resistivity of the deposited layers. Upon formation of the film, the electrode was removed and rinsed in distilled water. The switching characteristics were then studied by cycling the electrode in a 1M KOH solution at a potential sweep rate of 100 mV/sec. Samples were made in both the bleached and colored states and then immediately analyzed using spectroscopic techniques. It is important to note that upon removal of the electrode from its alkaline switching bath, the film would dehydrate after several hours, fading in color from bronze to transparent.

Spectral transmittance data were obtained to investigate the optical response of the films for both the bleached and colored states. The spectroscopic data included the ultraviolet (UV) and near-infrared (NIR) regions (200-3200 nm), where measurements were made by a Perkin-Elmer Lambda 9 spectrophotometer.

Backscattering spectrometry, using a Tandetron accelerator spectrometer (Cornell University), was performed on the nickel oxide thin film to analyze the chemical composition and film thickness. Two conditions were used, 3.0 MeV and 2.14 MeV He^{+2} with 20 uC of total charge, in a vacuum environment of 4×10^{-6} Torr. Additional cyclic voltammetry performed on the nickel oxide electrodes involved examining the films at various potential sweep rates from 5-150 mV/sec and electrolyte concentrations of 1M-0.0001M KOH + KCL supporting electrolyte.

Fourier-transform infrared spectroscopy (IBM-98 spectrometer) was used to study the molecular structure of the anodically deposited nickel oxide films in the far and mid-infrared regions for both the colored and bleached states. The films were analyzed in a reflection configuration, but the data were converted to effective single-pass transmittance by computer simulation. The measurements were performed at an atmosphere of 10^{-3} Torr in a nitrogen environment. These experiments helped in characterizing the reaction mechanism.

RESULTS AND DISCUSSION

A variety of experimental techniques were used to characterize the hydrated nickel oxide electrochromic electrode. Optical spectrophotometry revealed the electrode's optical absorption properties. Ion-backscattering spectrometry aided in determining layer thickness and chemical composition in dehydrated (bleached) films. Extensive voltammetry experiments helped us to understand the mechanism of coloration in the films and to determine the electrochemical nature of the films. Fourier-transform infrared spectroscopy helped to further identify the molecular vibrations of species formed after coloration or bleaching.

The nickel oxide thin films were anodically deposited onto the tin oxide-coated glass electrodes. The glass electrode was analyzed in prior work[12] by sputter Auger and X-ray photoelectron spectroscopy, with results showing that the composition was SnO_2:F, Cl.

Optical Spectroscopy

The solar and visible transmittances of the bleached and colored nickel oxide electrodes were measured using a spectrophotometer. For this study, the nickel oxide films were anodically deposited by electrochemical techniques and then cycled in an alkaline bath to obtain the colored and bleached states. The film thickness was 500 Å. The optical spectra are depicted in figures 2 and 3 for the visible and solar spectra, respectively. Integrating with respect to the solar (AM2)[14] and photopic (human-eye-visible response) spectra[15], the photopic and solar transmittances are: T_p (bleached)= 0.77, T_p (colored)= 0.21, T_S (bleached)= 0.73, and T_S (colored)= 0.35. By integrating separately the solar (AM2) near-infrared region, the value is T_{NIR} (colored)= 0.55 and T_{NIR} (bleached)= 0.72. In addition, the transmittance of the tin oxide-coated glass was measured to be T_S = 0.74, T_p = 0.80, and T_{NIR} = 0.71. Thus, in the bleached state, the nickel oxide does not significantly change the optical properties of the tin oxide-coated glass.

Backscattering Spectrometry

Backscattering spectrometry was performed on the nickel oxide film in the bleached state to determine its chemical composition and thickness. The two samples examined were prepared under identical conditions. (See preceeding description of experimental procedures.) Figures 4 and 5 are spectra of the substrate and film (which included the conductive SnO_2:F, Cl layer and substrate), respectively, where the charged alpha particles at 3 MeV were incident at 7 ° from the sample normal in an environment of 4 x 10^{-6} torr. The substrate was found to contain the elements O, 1.07 MeV; and Si, 1.69 MeV. (See Figure 4.) The film, along with the conductive layer and substrate, was composed of O, 1.07 MeV; Si, 1.56 MeV; Cl, 1.89 MeV; Ni, 2.30 MeV; and Sn, 2.69 MeV. (See Figure 5.) The data obtained correlated with standard tabulated values[16].

Figure 6 is another backscattering spectrum of the nickel oxide film, showing better depth resolution and an improved signal-to-noise ratio, where the charged alpha particles were generated with 2.14 MeV at 60 ° from normal incidence in an environment of 4 x 10^{-6} torr. The elemental composition was O, 0.78 MeV; Cl, 0.93 MeV; Ni, 1.64 MeV; and Sn,1.88 MeV, again in agreement with standard values[16]. Backscattering spectrometry gave data consistent with that of Auger and x-ray photoelectron spectroscopy of previously studied identical films[12]. In addition, the compositions of the nickel oxide film and

the conductive layer were accurately determined[17] to be $NiO_{1.0}$: $Cl_{0.026}$ with a thickness of 125 Å and, $SnO_{1.9}$:F, Cl with a thickness of 4400 Å (fluorine was determined by X-ray photoelectron spectroscopy), respectively.

Cyclic Voltammetry

The first set of cyclic voltammetry experiments was performed using a periodically increasing triangular potential on the anodic half-cycle. The experimental conditions included 1M KOH as an electrolyte at a sweep rate of 50 mV/sec. The starting potential was -500 mV in all cases. The anodic limit was +300 mV for cycle 1, and it was increased 100 mV on each subsequent cycle, ultimately being fixed at +750 mV. After eight cycles, the electrode was allowed to cycle between -500 mV and +750 mV, to a total of fifty cycles. However, after the sixth cycle (600 mV anodic potential), very little change was noted. These results are shown in Figure 7. The electrode response is very similar to that noted for oxidized metallic nickel electrodes[12]. The specific characteristics noted in this voltammogram (Figure 7) are a single predominant anodic peak at 390 mV (SCE) and a single predominant cathodic peak at 190 mV (SCE). Also, an oxygen-evolution peak occurs at about 550 mV (SCE). Similar results have been noted by other investigators (18-20). The oxidation reaction taking place at the anodic peak has been identified as $Ni(OH)_2 \rightarrow NiOOH + H^+ + e^-$. At the cathodic peak the reduction reaction has been determined to be $NiOOH + H^+ + e^- \rightarrow Ni(OH)_2$. In Figure 7, it should be noted that during the third to sixth cycles, there is a slight increase in the cathodic peak current. This increase tends to indicate that under the conditions of this low sweep rate the NiOOH is not completely reduced to $Ni(OH)_2$ during these first few cycles. The cathodic peak potential did not change during these early cycles, indicating stability of the film even though the oxygen-evolution potential had been exceeded. The distinct phases noted by other investigators for the alpha and beta forms of $Ni(OH)_2$ and the alpha and beta forms of NiOOH were not noted in this work[11,21,23].

Potential-scan experiments were carried out under sweep rates of 5-150 mV/sec in 1M KOH electrolyte. From these experiments, information regarding the effect of proton diffusion on the reaction can be obtained. The results of the potential scan are shown in Figure 8. By plotting the peak current density versus the square root of the sweep rate, as shown in figures 9 and 10, a linear relationship is found, which implies that the reaction is purely diffusion controlled. To determine if the diffusion of the proton was controlling the reaction, the concentration of hydroxyl ions was varied from 1M to 0.001M with KOH. A supporting electrolyte of KCL was used to keep the electrolyte conductivity constant. The anodic peak current results for these different electrolyte concentrations are shown in Figure 9. From these data, it is noted that the slopes of the curves, which are a function of the diffusion coefficient of a single ion species, do not depend on hydroxide ion concentration. Work by others has identified this ion as a proton[11,18-22]. Therefore, the proton must be the significant ion in the rate-determining process for both the anodic and cathodic cycles, at least in the electrolyte-concentration range studied. The maximum proton-diffusion coefficient has been determined for thicker films (1-1.8 um) by semi-infinite and finite diffusion models. For those films, the diffusion coefficient was estimated to be in the range of 10^{-10} -10^{-11} cm^2 sec^{-1} with a diffusion length of 0.55 um[21,22]. The films used in this experiment are too thin to be applicable to these diffusion models.

Fixed-sweep, variable-electrolyte-concentration experiments were conducted to determine if a very low concentration of hydroxyl ions influences the proton-reaction mechanism. The range of electrolyte concentrations was 1M to 0.0001M KOH, with KCl added to keep conductivity constant, where the sweep rate of 50 mV/sec was used. The results are shown in figures 11 and 12. The reversible potential for $Ni(OH)_2 \longleftrightarrow NiOOH + H^+ + e^-$ is shown in Table 1 for different electrolyte concentrations. There is an overall trend of anodic and cathodic peaks shifting to higher potentials for lower concentrations, resulting in higher reversible potentials. This effect has been noted in KOH and other electrolytes by other investigators[21,24]. This result demonstrates that the concentration of surface OH^- groups has a significant impact on the movement of protons diffusing within the films to the film-electrolyte interface. Also, this experiment shows that generally the concentration of hydroxyl ions has no significant role in the anodic oxidation of nickel hydroxide, suggesting that the diffusion of the proton is the rate-limiting process.

To understand further the role of surface hydroxyl groups, we compared the electrochemical switching of these films as they were alternated between neutral and highly alkaline electrolytes. The beginning experiment used a 1M KCl electrolyte, which gave no voltammetric response. When the film was transferred and cycled in 1M KOH the oxidation and reduction peaks shown in Figure 13A appeared. The film was next removed at a potential above the coloration peak and transferred to 1M KCl; a reduction peak was seen only for the first cycle. (See Figure 13B.) This demonstrates that the hydroxyl ions must be present at the film surface for oxidation to occur. In another experiment, the film electrode was removed from 1M KOH in the bleached state and transferred to 1M KCl where 1M HCl was also added. During cycling, no anodic or cathodic peaks were observed, as noted in Figure 13C. The film was then cycled in 1M KOH and showed the oxidation/reduction peaks (Figure 13D), indicating that the film remained at the electrode surface. This shows that oxidation cannot occur in the absence of hydroxyl ions.

Fourier-Transform Infrared Spectroscopy

Fourier-transform infrared (FTIR) spectroscopy was used to probe the composition and structure of the film in both colored and bleached states. The anodically deposited nickel oxide was soaked in distilled water, transferred to 1M KOH solution, and potentiostatically cycled ten times between -500 mV and +750 mV (SCE), after which alternating coloration and bleaching states were observed. The cycling was first interrupted with the film in its colored state, i.e., at a potential higher than the anodic peak potential. Then the electrode was washed with distilled water and transferred to the FTIR spectrometer. The IR spectra of the sample shown in figures 14 and 15 were collected at 10^{-3} Torr. Next, the cycling was interrupted with the film in its bleached state, at a potential lower than the cathodic peak potential, and a spectrum was taken for the film in its bleached state. The IR peaks between 3000 cm^{-1} and 4000 cm^{-1} show the OH stretch and combination modes of OH in H_2O. The 450 cm^{-1} to 560 cm^{-1} peaks in Figure 15 belong to the nickel-oxygen stretch and out-of-plane deformation of surface OH bonds. The spectra show several types of OH groups, hydrogen-bonded and lattice water with different elastic force constants. There is a small contribution of the OH bond associated with the bleached state compared to the colored film. At wave numbers greater than 3400 cm^{-1},

there is also an indication of the presence of water in the lattice, even under a 10^{-3} Torr vacuum atmosphere. FTIR spectras of the film after aging in vacuum for two days indicate partial decomposition of hydrated NiOOH to hydrated $Ni(OH)_2$ with fewer water molecules.

Electrochromic Switching Mechanism

The proposed mechanism for this reaction is the following: increasing the anodic potential reduces the energy barrier for oxidation of Ni(II) to Ni (III), thereby increasing the interaction of Ni (II) with OH ions. This results in a situation that weakens the OH bond and tends to increase the mobility of the proton. At anodic oxidation potentials, the charge transfer takes place and Ni (II) is transformed to Ni (III), while protons are released from the OH group. (See Figure 16.) The diffusion of the released protons through the film is rate-limiting in this process. The diffusing protons will react with OH ions at the electrode/electrolyte interface to form water molecules. The mechanism, depicted in Figure 16, is the most probable pathway for the electrochromic transformation of the deposited nickel oxyhydroxide.

CONCLUSIONS

From the results obtained in these experiments, the authors conclude that hydrated nickel oxide thin films exhibit favorable switching properties for application in architectural glazings. The optical properties of the NiO/SnO_2:F, Cl/glass electrode were T_p(bleached) = 0.77, T_p(colored) = 0.21, T_S(bleached) = 0.73, and T_S(colored)= 0.35 for film thickness of 500 Å. Ion-backscattering experiments determined the composition of a 125 Å dehydrated nickel oxide film to be $NiO_{1.0}$. Anodic deposition onto the doped tin oxide-coated glass in 0.1M $NiSO_4$ + 0.1M NH_4OH resulted in the formation of the nickel oxyhydroxide film. The electrochemical properties of both the bleached and colored states were determined by cyclic voltammetry, indicating that the reversible reaction is $Ni(OH)_2 \longleftrightarrow NiOOH + H^+ + e^-$. The reversible process between bleached and colored states involves solid-state diffusion of the proton through the film, where the hydroxyl ion plays an important role in the reaction mechanism. Fourier-transform infrared spectroscopy was performed on the anodic film, where lattice water and hydroxyl groups in several different bonding environments were found. Future investigations using in-situ FTIR are expected to more fully explain the structure and its relation to the coloration and bleaching properties.

ACKNOWLEDGEMENTS

The authors wish to thank A.J. Yu (Cornell University, Ithaca, N.Y.) for his dedicated efforts with the backscattering spectroscopy work, and Drs. D. McArthur, D. Corrigan, and D. Snyder for their analysis of the electrochemical results. Special thanks goes to S. Selkowitz, Prof. J. Washburn, and Dr. T. Sands (Bell Communications Research, Inc., Murray Hill, N.J.) for their support. We would like to thank Bruce Mayer (Watkins-Johnson, Scotts Valley, CA) for supplying the conductive glass. The work was performed at Lawrence Berkeley Laboratory, Materials and Molecular Research Division, under a joint program with the Applied Science Division. The work was funded in part by the Assistant Secretary for Conservation and Renewable Energy, Office of Solar Heat Technologies, Solar Buildings Division of the U.S. Department of Energy under Contract No. DE-AC03-76SF00098.

REFERENCES

1. Johnson, R., Connell, D., Selkowitz, S., and Arasteh, D., "Advanced Optical Materials for Daylighting in Office Buildings," in *Proc. of 10th National Passive Solar Conf.,* Oct. 1985, Raleigh, N.C.

2. McIntyre, J. D., Peak, W. F., and Schwartz, G. P., "Electrochromism in Hydrous Nickel Oxide Films," Electronic Materials Conference, Abstract D-4. 1979.

3. Lampert, C. M., "Electrochromic Materials and Devices for Energy Efficient Windows," *Solar Energy Materials,* Vol. 11, p. 1. 1982.

4. Dautrement-Smith, W. C., "Transition Metal Oxide Electrochromic Materials and Displays: A Review," *Displays,* Vol. 4, p. 367. 1982.

5. Faughnan, B.W., and Crandall, R. S. "Electrochromic Displays based on WO3," in *Topics in Applied Physics,* Vol. 40, ed. J.I. Pankove, Berlin: Springer-Verlag. 1980.

6. Goldner, R.B., et al., "High Near Infrared Reflectivity Modulation with Polycrystalline Electrochromic WO3," *Appl. Phys. Lett.,* Vol. 43, p. 1093. 1983.

7. Gunther, R., and Gross, S., eds., "*Proceedings of the Symposium on the Nickel Electrode,*" The Electrochemical Society, Battery Division, Vol. 82-84. 1984.

8. Tuomi, D., "The Forming Process in Nickel Positive Electrodes," *J. Electrochemical Soc.,* Vol. 112, p. 1. 1965.

9. Mandandhav, K., and Pletcher, D., "The Preparation of High Surface Area Nickel Oxide Electrodes for Synthesis," *J. of Appl. Electrochem.,* Vol. 9, p. 707. 1979.

10. Kober, P., "Analysis of the Charge-Discharge Characteristics of Nickel Oxide Electrodes by Infrared Spectroscopy," *J. Electrochem. Soc.,* Vol. 112, p. 1064. 1965.

11. Olivia, P., Leonaredi, J., and Laurent, J. F., "Review of the Structure and the Electrochemistry of Nickel Hydroxide and Oxyhydroxides," *J. Power Sources,* Vol. 8, p. 229. 1982.

12. Lampert, C. M., Omstead, T. R., and Yu, P. C., "Chemical and Optical Properties of Electrochromic Nickel Oxide Films," in *Proc. of SPIE,* Vol. 562, p. 15. 1985.

13. Lampert, C. M., "Materials Chemistry and Optical Properties of Transparent Conductive Thin Films for Solar Energy Utilization," *Ind. Eng. Chem. Prod. Res. Dev.,* Vol. 21, p. 612. 1982.

14. Bird, R. E., and Hulstrom, R. L., "Additional Solar Spectral Data," *Solar Cells,* Vol. 8, p. 85. 1983.

15. Barnes, F. A., ed., *RCA Electro-Optics Handbook,* Harrison, N.J.: RCA Corporation. 1974.

16. Doolittle, L., "Algorithms for the Rapid Simulation of Rutherford Backscattering Spectra," *Nuc. Instrum. Methods,* Vol. B9, p. 344. 1985.

17. Chu, W. K., Mayer, J. W., and Nicolet, M. A., *Backscattering Spectrometry.* London: Academic Press. 1978.

18. Schrebler-Guzman, R.S., Vilche, J. R., and Arvice, A. J., "The Potentiodynamic Behavior of Nickel in Potassium Hydroxide Solutions," *J. Appl. Electrochem.,* Vol. 8, p. 67. 1978.

19. Weininger, J. L., and Breiter, M. W., "Hydrogen Evolution and Surface Oxidation of Nickel Electrodes in Alkaline Solutions," *J. Electrochem. Soc.,* Vol. 111, p. 707. 1964.

20. Schrebler-Guzman, R.S., Vilche, J.R., and Arvia, A.J., "The Kinetics and Mechanism of the Nickel Electrode III: The Potentiodynamic Response of Nickel Electrodes in Alkaline Solutions in the Potential Region of Ni(OH)2 Formation," *Corrosion Science,* Vol. 18, p. 765. 1977.

21. MacArthur, D.M., "The Hydrated Nickel Hydroxide Electrode Potential Sweep Experiments," *J. Electrochem Soc.,* Vol. 117, p. 422. 1970.

22. MacArthur, D. M., "The Proton Diffusion Coefficient for Nickel Hydroxide Electrode," *J. Electrochem. Soc.,* Vol. 117, p. 729. 1970.

23. Bode, H., Dehmelt, K., and Nitte, J., "Zur Kenntnis der Nickelhydroxidelektrode-I uber das Nickel (II) Hydroxidhydrat," *Electrochem. Acta,* Vol. 11, p. 1074. 1966.

24. Barnard, R., Randell, C. F., and Tye, F. L., "Studies Concerning Charged Nickel Hydroxide Electrodes IV: Reversible Potentials in LiOH, NaOH, RbOH, and CsOH," *J. Appl. Electrochem.,* Vol. 11, p. 517. 1981.

TABLE 1

REVERSIBLE POTENTIAL OF
$Ni(OH)_2 \leftarrow\rightarrow NiOOH = H^+ + e^-$

FOR VARIOUS CONCENTRATIONS OF KOH AND CONSTANT

ELECTROLYTE CONDUCTIVITY.

Reversible Potential (V) vs SCE	KOH Concentration (M)
2.4	1.00
3.14	0.5
3.50	0.2
3.70	0.1
3.90	0.005
4.40	0.001
4.90	0.0005
5.22	0.0001

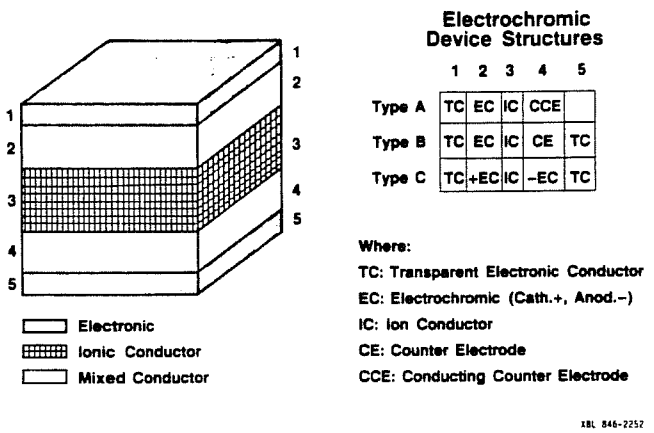

Figure 1. Schematic cross section of a generalized electrochromic device.

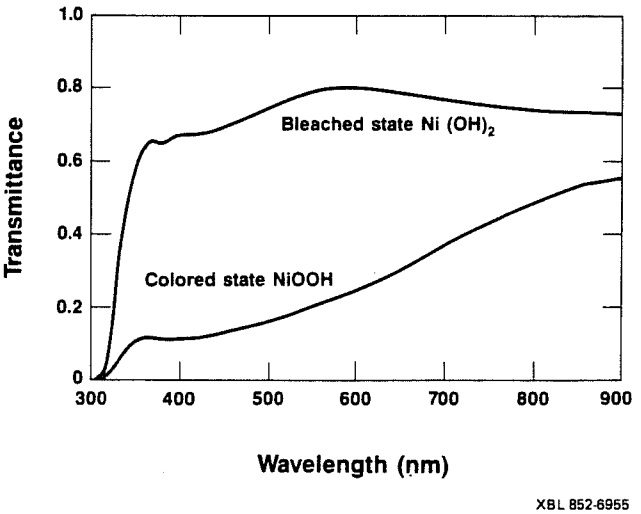

Figure 2. Normal spectral visible transmittance of electrochromic NiO/SnO_2:F,Cl/glass.

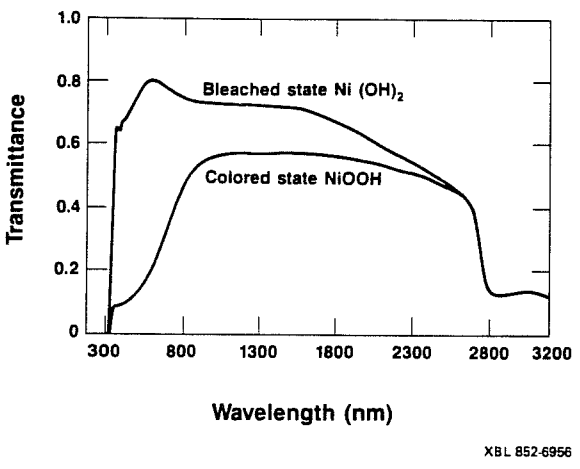

Figure 3. Normal spectral solar transmittance of electrochromic NiO/SnO_2:F,Cl/glass.

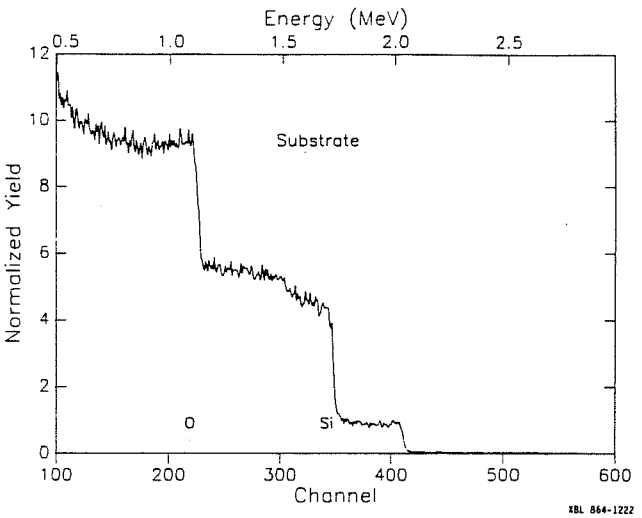

Figure 4. Ion-backscattering spectrum of substrate. Principle chemical elements identified are 0, 1.07 MeV; and Si, 1.69 MeV.

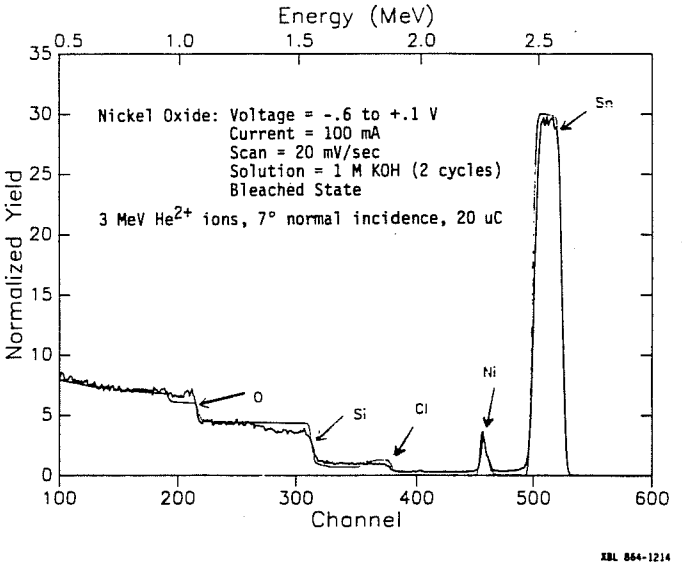

Figure 5. Ion-backscattering spectrum of NiO/SnO_2: Cl/glass electrode. Principle chemical elements identified are O, 1.07 MeV; Si, 1.56 MeV; Cl, 1.89 MeV; Ni, 2.30 MeV; and Sn 2.69 MeV.

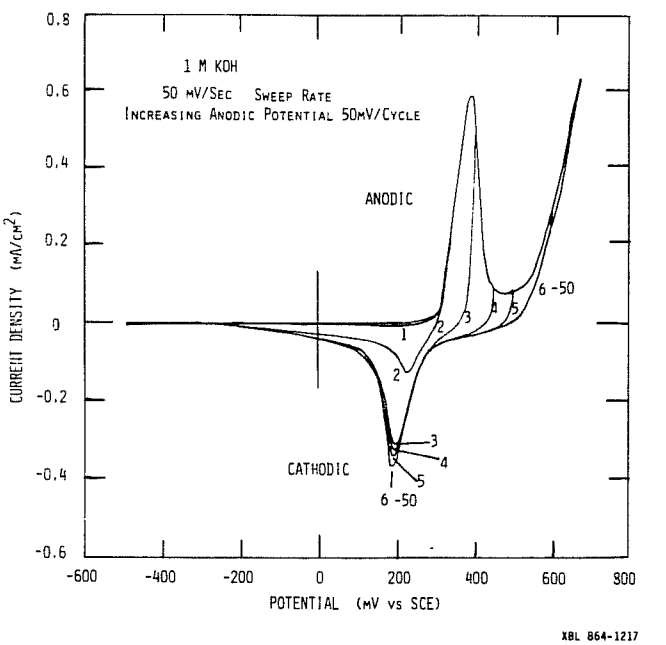

Figure 7. Cyclic voltammogram of NiO/SnO_2:F, Cl/glass electrode in 1M KOH at a sweep rate of 50 mV/sec.

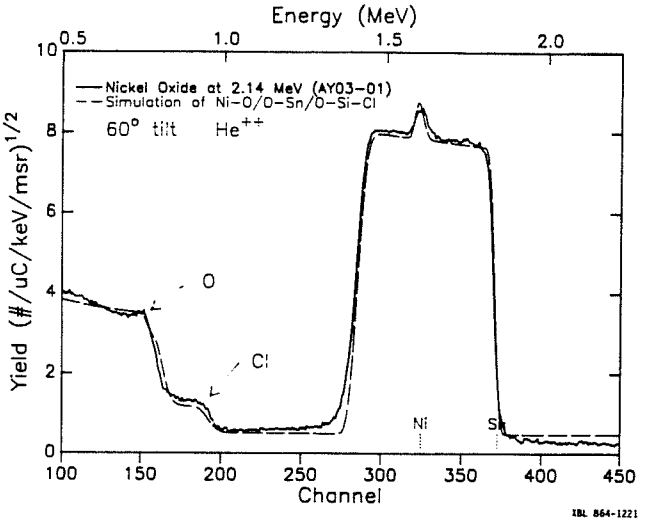

Figure 6. Ion-backscattering spectrum of NiO/SnO_2: Cl/glass electrode. Principle chemical elements identified are O, 0.78 MeV; Cl, 0.93 MeV; Ni, 1.64 MeV; and Sn, 1.88 MeV.

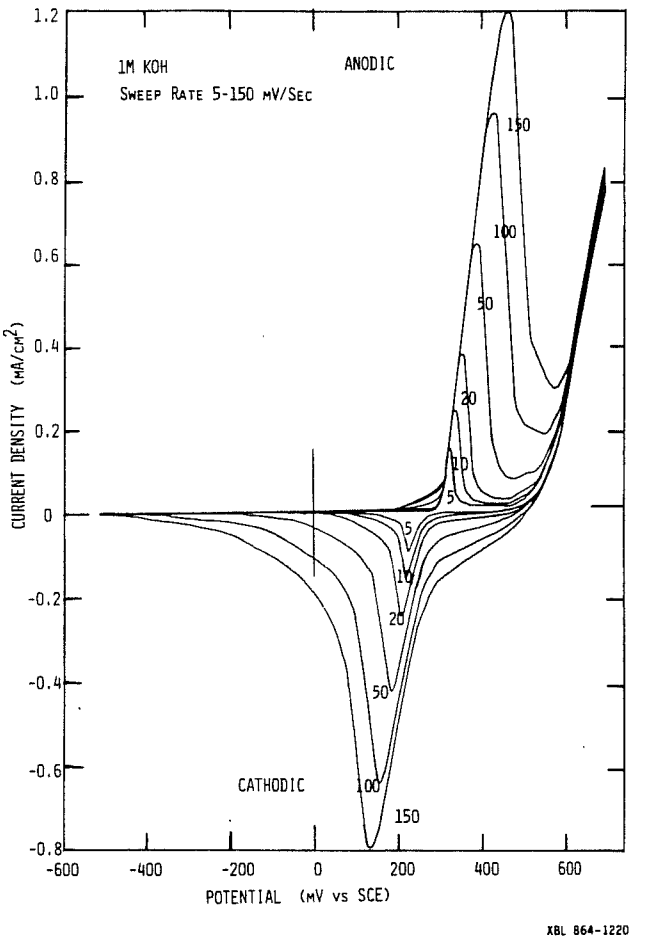

Figure 8. Cyclic voltammogram of NiO/SnO_2:F, Cl/glass electrode in 1M KOH at various potential sweep rates. The number on each voltammogram represents the sweep rate (mV/sec).

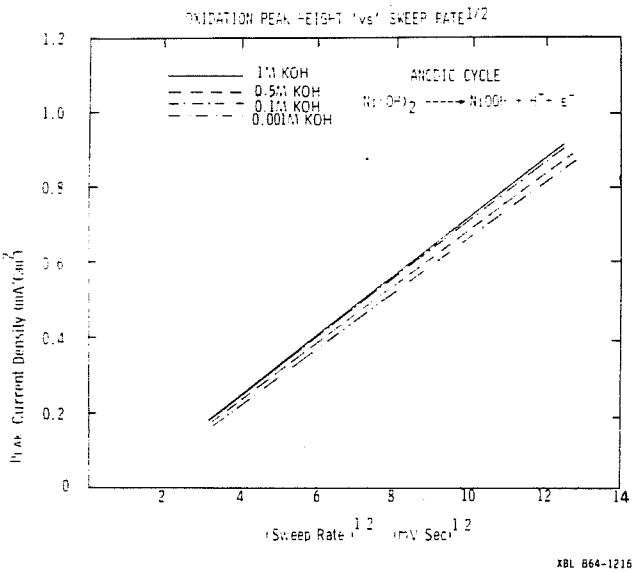

Figure 9. Anodic peak current densities for the coloration of the NiO/SnO_2:F,Cl/glass electrode system vs. (sweep rate)$^{1/2}$ for various concentrations of KOH, ranging from 0.001M to 1M KOH.

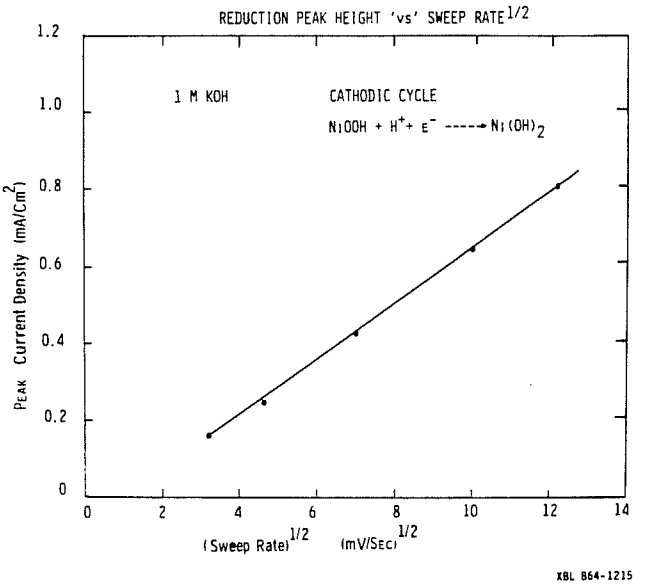

Figure 10. Cathodic peak current densities for the bleaching of the NiO/SnO_2:F, Cl/glass electrode system vs. (sweep rate)$^{1/2}$ for 1M KOH.

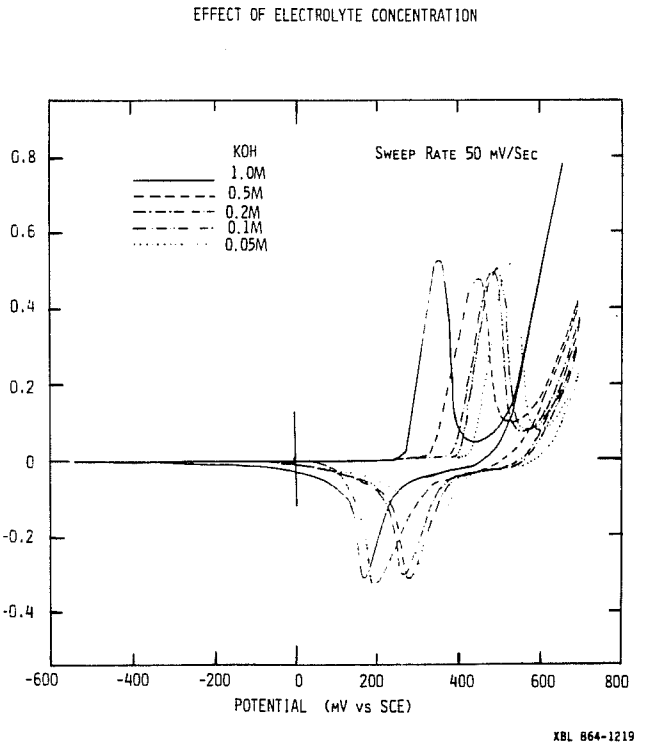

Figure 11. Cyclic voltammogram of NiO/SnO_2:F,Cl/glass electrode at a fixed sweep rate of 50 mV/sec in various concentrations of KOH, ranging from 0.5M to 1M.

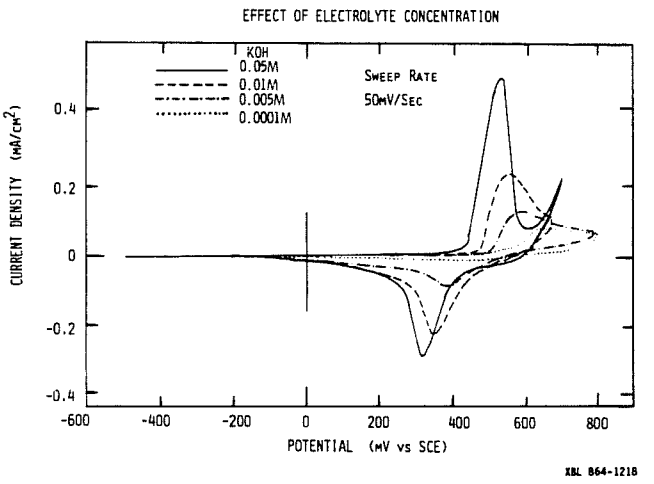

Figure 12. Cyclic voltammogram of NiO/SnO_2:F, Cl/glass electrode at a fixed sweep rate of 50 mV/sec in various concentrations of KOH, ranging from 0.0001M to 0.05M.

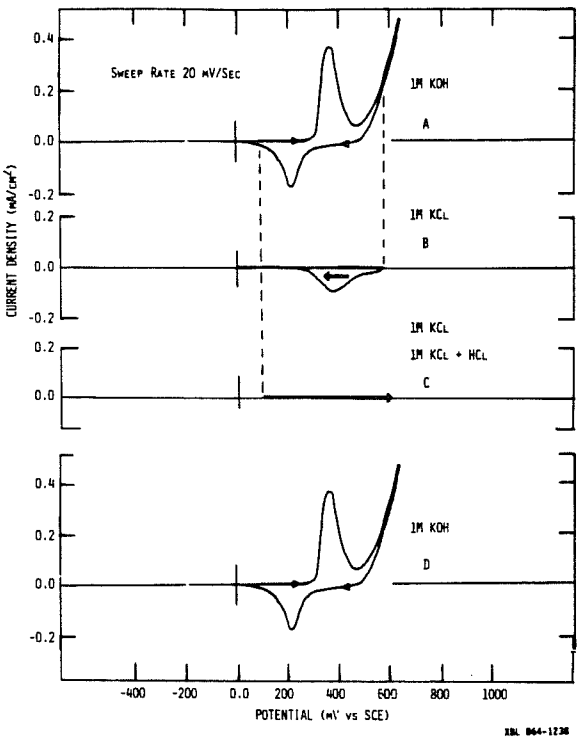

Figure 13. Cyclic voltammogram of NiO/SnO_2:F, Cl/glass electrode at a fixed sweep rate of 20 mV/sec, in A) 1M KOH, B) 1M KCl, C) 1M KCl + HCl, and D) 1M KOH.

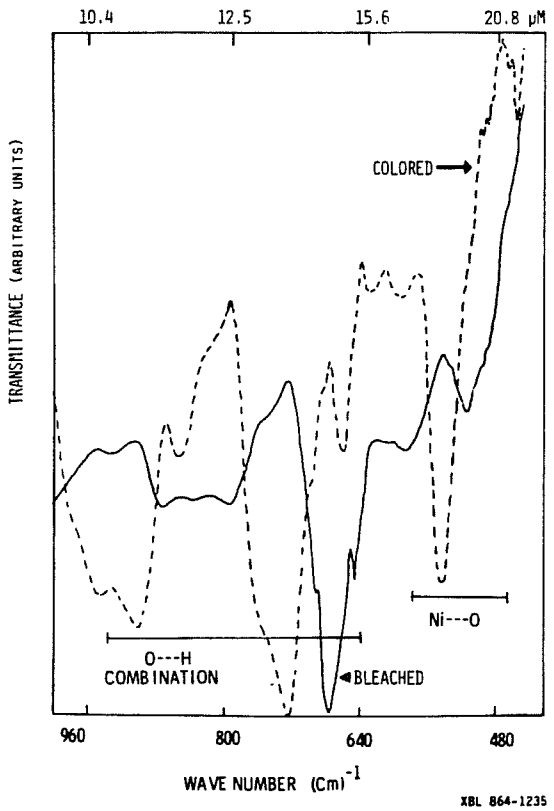

Figure 15. Fourier-transform infrared reflection spectrum (mid-IR) of a bleached anodically deposited nickel oxide film, cycled in a 1M KOH solution.

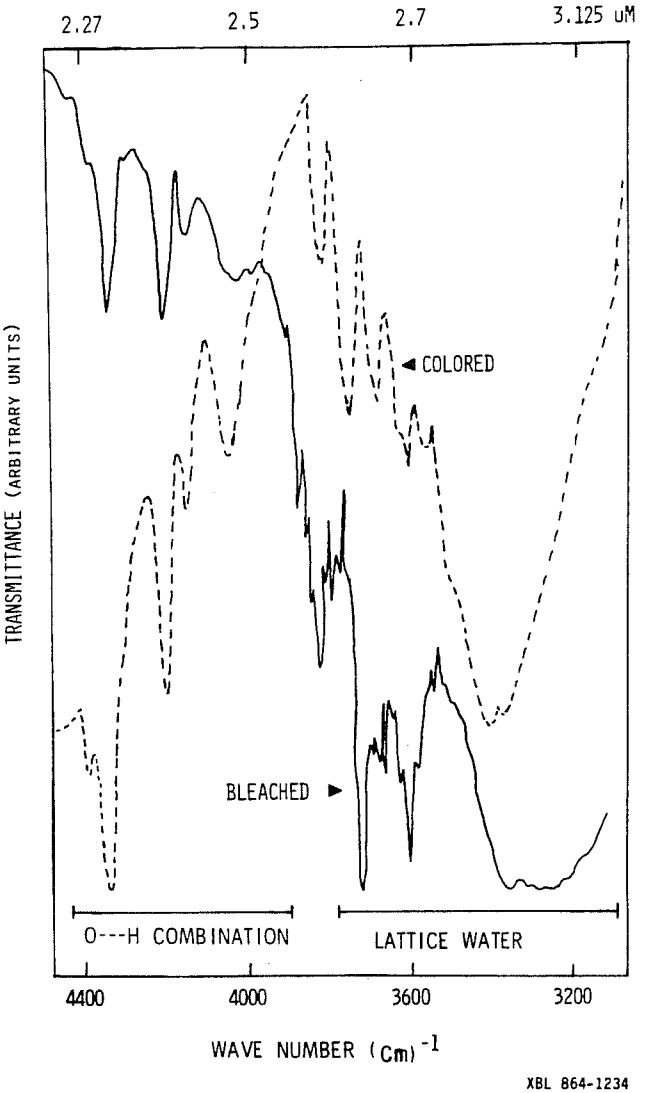

Figure 14. Fourier-transform infrared reflection spectrum (near-IR) of an anodically deposited nickel oxide film, cycled in a 1M KOH solution.

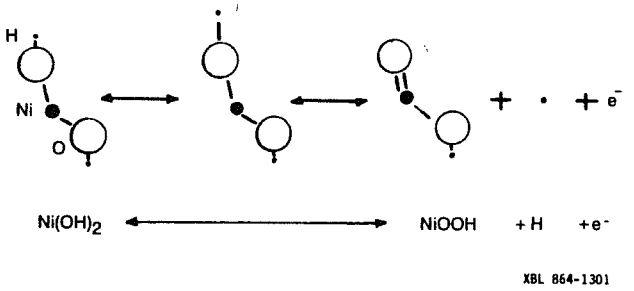

Figure 16. Proposed electrochromic switching mechanism for the deposited nickel oxyhydroxide.